Notes

Sequential Sea-ice Concentration Prediction for Marine Operations in Ice-Infested Waters

By M. El-Diasty and A. El-Rabbany, Department of Civil Engineering, Ryerson University, Canada

Marine operations in ice-infested waters require reliable and timely information about the sea ice conditions. The Canadian Ice Service produces and distributes the ice information to mariners operating in Canadian waters, mainly in the form of daily ice charts. Unfortunately, due to the time difference between the production and the use of the ice charts, the ice information is always out of date, which endangers the safety of marine operations. To efficiently overcome this problem, a reliable model for predicting the sea ice concentration over time is developed.

Examining the ice charts of the Gulf of St. Lawrence during the period 1987 to 1998 showed that the sea ice conditions change according to a regular pattern to some extent. Therefore, a neural network function approximation system could model, and hence predict, these changes efficiently when trained, using multiple-year ice concentration readings. Initially, the training was done in the batch mode. However, this was found inefficient when abrupt changes in the values of the ice concentration were encountered.

Therefore, a sequential model, which uses the modular neural network structure, was developed. In addition to overcoming the drawbacks of the batch method, the sequential model is more suitable for real-time applications.

Introduction

Marine operations in ice-infested waters require reliable and timely information about the sea ice conditions. Validation experiments have shown that radar remote sensing, particularly RADARSAT, has the capability of providing such comprehensive information. The ScanSAR modes of RADARSAT are recommended for comprehensive monitoring of the sea ice conditions. The Canadian Ice Service (CIS) is primarily using these modes, along with other sources of information such as airborne and other satellite remote sensing, for extracting the sea ice information in the form of daily ice charts (Ramsay et al., 1998; Canadian Ice Service, 1994). The ice charts contain information such as the ice concentration and type, ice edge location, icebergs and open leads. The total concentration of the sea ice is the most important element of the ice information required to support vessels with no ice capability (Haykin et al., 1994). Unfortunately, due to the time difference between the production and the use of the ice charts, the ice information is always out of date, which jeopardises the safety of marine operations (Canadian Ice Service, 2001). To efficiently overcome this problem, a neural network-based model is developed for sequentially predicting the sea ice concentration over time. A supervised neu-

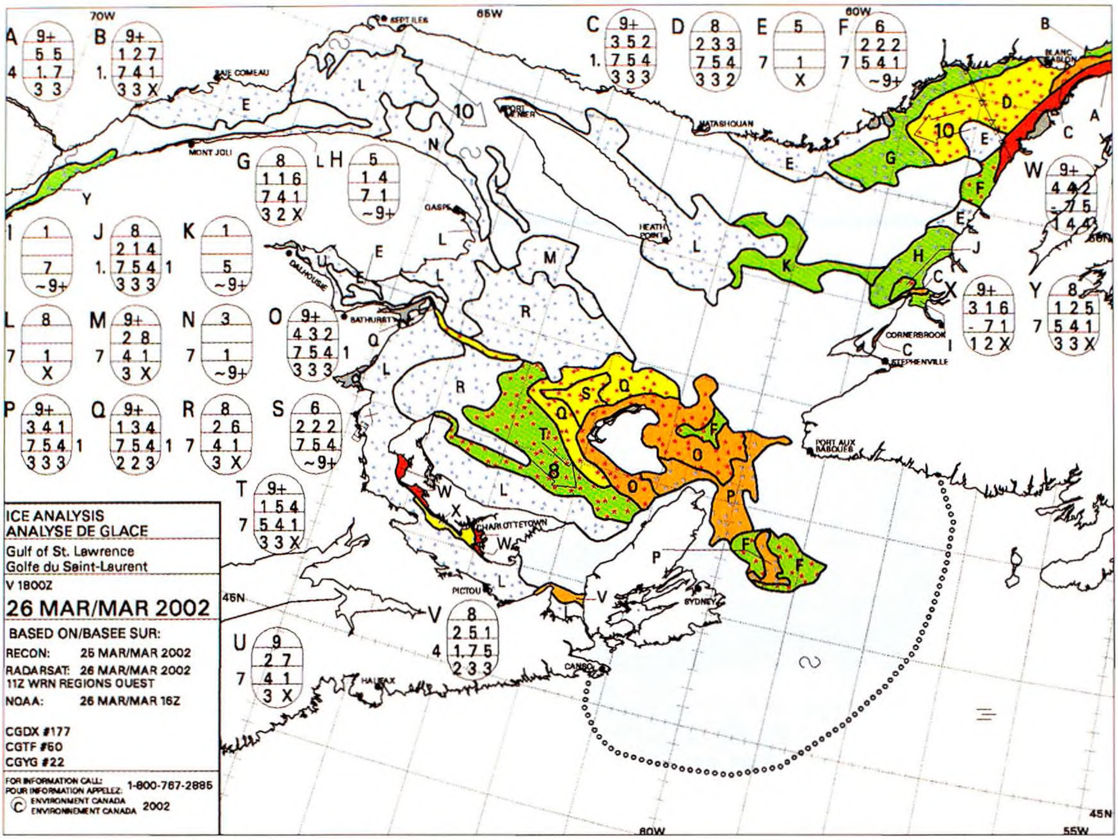

Figure 1: An example of the CIS ice chart for the Gulf of St. Lawrence

ral network is trained to predict the ice concentration at a given location and time using the CIS's ice charts. The input to the network is a vector which represents the current ice concentrations over a test area containing 40 points (see Figure 1). The input vector is mapped to an output vector that gives the predicted ice concentrations.

Production and Format of the Ice Charts

The Canadian Ice Service is responsible for providing the ice information in Canadian waters, mainly through its daily ice charts (Figure 1). To do this, the CIS uses various space-borne and airborne remote sensing sensors, shore station observations and shipboard ice observations (Canadian Ice Service, 1994). The charts use the North American Datum 1927 (NAD 27) and the Lambert conical projection. The World Meteorological Organization (WMO) symbolisation for ice information, frequently referred to as the 'Egg Code', is used to describe the ice conditions (Figure 1). Boundaries are drawn around the ice areas with different concentrations; each is represented by an egg code (Canadian Ice Service, 1994).

An egg code is an oval shaped symbol, which contains three parts that describe the concentration of the ice, the stage of development (age) of the ice concentration and the predominant form of ice (floe size). These are expressed by up to 12 numerical values. The concentration of the ice represents the ratio between the area of the water surface covered by ice and the total area, and is expressed in tenths. The value of the ice concentration varies from 10/10 for consolidated ice to 1/10 for open water. The single uppermost parameter in the egg code represents the total concentration, which includes all stages of development. The second row in the egg code matrix contains the partial concentration for the thickest (left), the second thickest (middle) and the third thickest (right) ice types. The partial concentration field may contain two numbers, if only two ice types are present in the area (see Figure 1). If there is one ice type only, the partial concentration field will be left

blank, as the concentration of the will be presented by the total concentration (Figure 1).
The third field in the ice code contains the stages of development (age) for the ice types reported in the partial concentration field. Thicker ice refers to older ice, and vice versa. Various codes are used, depending of the stage of development. For example, a code of '1' is a assigned to the new ice (less than 10 cm in thickness), while a code of '9' is assigned to the second stage thin first-year ice (50-70 cm in thickness). Medium/thick first-year ice as well as old ice are assigned a dot (·) as part of their code. The last field in the code represents the predominant forms of the sea ice (floe sizes) corresponding to the stages of development identified in the previous field. Various codes are given to various floe sizes, which vary from '0' for the pancake ice to '7' for the giant floe (width greater than 10 km). Fast ice and icebergs are given the codes of '8' and '9', respectively. Undetermined ice form, unknown or no form is assigned the code of 'X'.

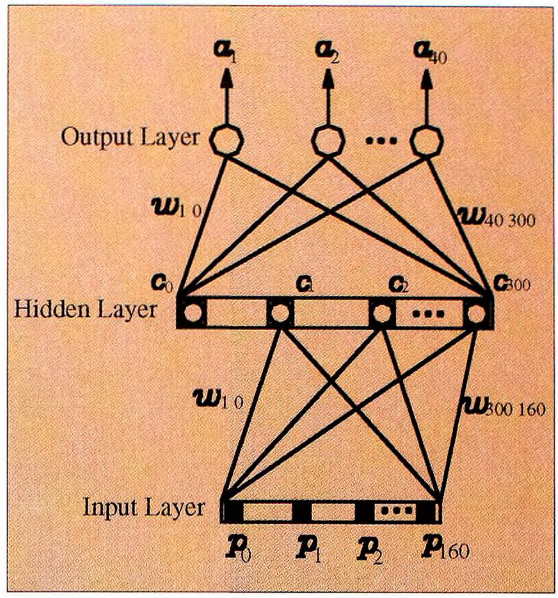

Figure 2: Three-layer feed-forward neural network with the structure [160-300-40]

Artificial Neural Network System

Artificial neural networks were used to build our computational model for the ice conditions because of their ability to learn from examples and 'generalise' on these examples. We chose the three-layer feed-forward neural network trained using the back-propagation algorithm for these experiments (Figure 2). The back-propagation algorithm uses gradient descent in weight space to minimize the output error. It converges to a locally optimal solution when an adequate number of input-output pairs of samples are subjected to the network for an adequate number of epochs. The back-propagation algorithm can be summarised in three steps as follows (see Abdelazim et al., 2001 and El-Rabbany et al., 2002 for more details). The first step is to propagate the input forward through the network. The neurons in the first layer receive external inputs:

$$\boldsymbol{a}^0 = \boldsymbol{p} \qquad (1)$$

$$\boldsymbol{a}^{m+1} = \boldsymbol{f}^{m+1}(\boldsymbol{W}^{m+1}\boldsymbol{a}^m + \boldsymbol{b}^{m+1}),$$

for *m* = *0, 1, ..., M-1* (2)

Where *M* is the number of layers in the network. Equation (1) provides the starting point for equation (2), and the output of the layer *m* is the input to the layer *m+1*. The outputs of the neurons in the last layer are considered the network outputs:

$$\boldsymbol{a} = \boldsymbol{a}^M \qquad (3)$$

The next step is to calculate the output error and back-propagate it to calculate the sensitivities (s values).

$$\boldsymbol{s}^M = -2\dot{\boldsymbol{F}}^M(\boldsymbol{n}^M)\,(\boldsymbol{t}-\boldsymbol{a}) \qquad (4)$$

$$\boldsymbol{s}^m = \dot{\boldsymbol{F}}^m(\boldsymbol{n}^m)\,(\boldsymbol{W}^{m+1})\,\boldsymbol{s}^{m+1}, \qquad (5)$$

for *m* = *M-1*, ..., 2, 1
Finally, the weights and biases are updated, based on the calculated sensitivities, using the approximate steepest descent rule:

$$\boldsymbol{W}^m(k+1) = \boldsymbol{W}^m(k) - \alpha\boldsymbol{s}^m(\boldsymbol{a}^{m-1})^T \qquad (6)$$

$$\boldsymbol{b}^m(k+1) = \boldsymbol{b}^m(k) - \alpha\boldsymbol{s}^m \qquad (7)$$

Where α is the step size. The three steps are repeated until the error reaches a minimum; hence, the calculated weights of the connections would represent the solution network.

Results for the Sea Ice Prediction

As mentioned above, a supervised neural network was trained to predict the ice concentrations at a randomly selected location within of the Gulf of St.

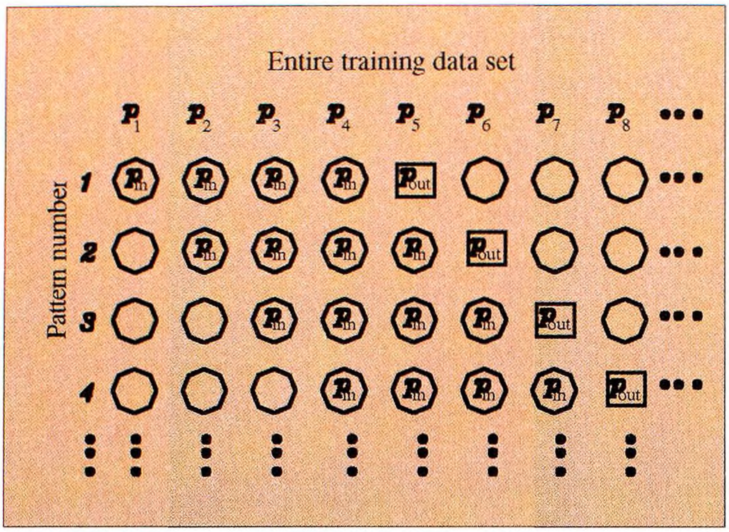

Figure 3: Training patterns used in the neural network input

Lawrence, which were provided by the Canadian Ice Service (CIS). The dataset consisted of the CIS's weekly ice charts over 11 years (1987-1998). The input ice data was mapped to an output vector that gave the predicted ice concentrations. The traditional non-modular feed-forward neural network structure failed to map the required function, and hence, was modularised to give better prediction performance. The structure of the neural network was built using the NeuralWare software (NeuralWare, 2001). Several tests were conducted to optimize the structure of the neural network. It was concluded that the modular neural network with the structure [160-300-5-40] gives the best results, i.e., has the lowest Root-Mean-Square (RMS) error. This structure represents 160 source neurons, 300 hidden neurons for both the local experts and the gating network, 5 'gating' output neurons, and 40 network output neurons.

Initially, we used the time (i.e., week number) as the only input to the network, which is usually followed in the literature (see, for example, El-Rabbany et al., 2002). However, although the trained network represented the training dataset reasonably well, the network prediction was rather poor due to the abrupt changes in the values of the ice concentration over short period of time (see Figure 5 below). Therefore, we followed another approach, which was proposed by Schuh et al. (2002). In this approach, the immediate past values of the ice concentration are used as input to the network, while future values of the ice concentration are used as the desired (i.e., actual) output. In the subsequent epochs, the training patterns are time-shifted as shown in Figure 3. Based on the size of the available dataset, a total 599 different patterns were created.

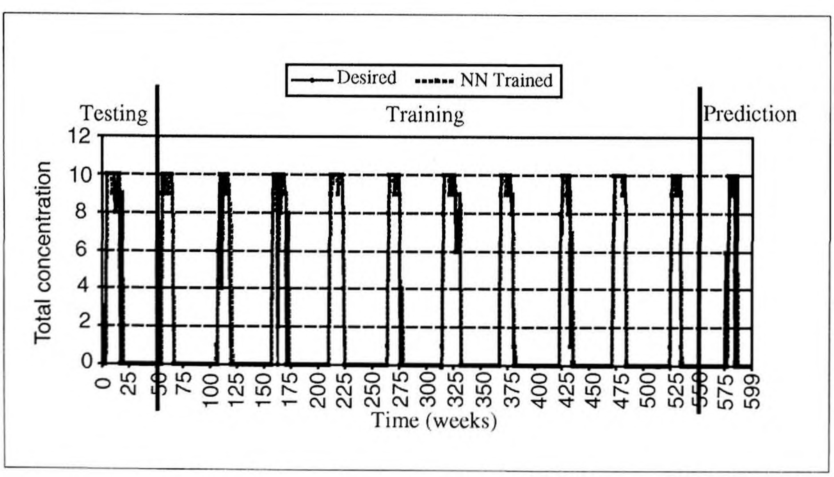

Figure 4: Selection of testing, training and validation data subsets

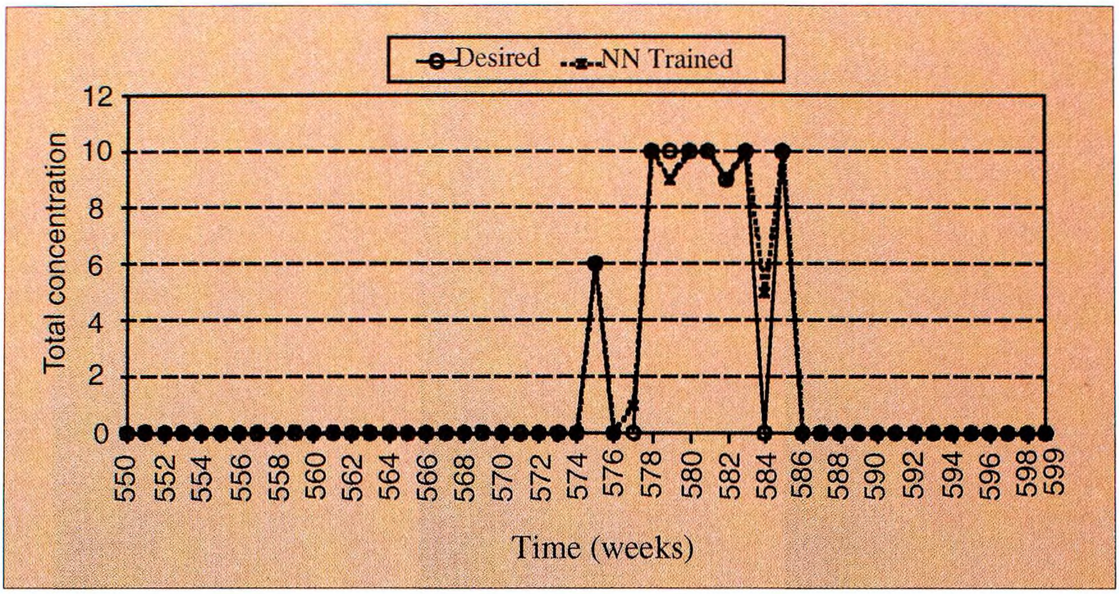

Figure 5: Actual versus predicted ice concentration values for the year 1998

The dataset was divided into three subsets: training, testing and validation subsets (Figure 4). The first 50 patterns were assigned to the testing subset, while the last 50 patterns were assigned to the validation subset. The training subset was selected to represent the middle portion of the dataset, i.e., 499 patterns. The training was stopped based on testing the generalization performance of the neural network using the testing subset. After training and testing the network, we generalized the model to predict ahead the last 50 patterns of the dataset and compared the results with the actual values of the ice concentration. This was done in a sequential manner to emulate the real-time condition. Figure 5 shows the predicted ice concentration values versus the desired values.

The performance of the network was measured based on the percentage of correct prediction, i.e., the ratio of the correct network output values and the actual values at the various points in the test area. The network solutions show that the prediction performance of the neural network varied between 86 per cent (43 out of 50 were correct) and 98 per cent (49 out of 50 were correct). The average overall performance of the network over the entire test area (i.e., over the 40 points) was 93.2 per cent. This shows that, despite the fact that the environmental conditions were not included, the neural network was capable of predicting the ice concentration at high prediction accuracy level. Figure 5 shows the actual versus predicted ice concentrations for the year 1998, at a randomly selected point within the test area.

Conclusions and Future Work

A sequential neural network-based model for ice concentration prediction was developed in this paper. The modular neural network structure gave the best performance results (i.e., the minimum RMS), and therefore was used in predicting the ice concentration values at a selected test area within the Gulf of St. Lawrence. It is shown that, despite the absence of the environmental data, the prediction performance of the neural network varied between 86 per cent and 98 per cent. The average overall performance of the network over the entire test area (i.e., over the 40 points) was 93.2 per cent. To further enhance the prediction capability, a future version of the model will include environmental data and other ice parameters, e.g., the partial ice concentrations and the stages of development of the ice types.

Acknowledgments

This research is supported by the Centre for Research in Earth and Space Technology (CRESTech), an Ontario Centre of Excellence. The ice charts were provided by the Canadian Ice Service (CIS) in Ottawa.

References

Abdelazim, S., A. El-Rabbany and G. Auda (2001). '*Artificial Neural Networks for Ice Concentration Prediction.*' Accepted for Publication at the Journal of Marine Geodesy

Canadian Ice Service (1994). '*MANICE: Manual of Standard Procedures for Observing and Reporting Ice Conditions.*' Environment Canada, Ottawa, Canada

Canadian Ice Service (2001). '*ECDIS Ice Objects*', Version 3.0, Environment Canada, Ottawa, Canada

El-Rabbany, A. (2000). '*Integrated Navigation Chart System.*' Invited presentation at the 'Ice in ECDIS' Workshop, St. John's, Newfoundland, 5-6 June

El-Rabbany, A., G. Auda and S. Abdelazim (2002). '*Predicting Sea Ice Conditions Using Neural Networks.*' Journal of Navigation, Vol. 55, Number 1, pp. 137-143

Haykin, S., E.O. Lewis, R.K. Raney and J.R. Rossiter (1994). *Remote Sensing of Sea Ice and Icebergs*, John Wiley & Sons, Inc

NeuralWare Inc. (2000). '*NeuralWorks II/Plus: Software Manual*', PA, USA

Ramsay, B., M. Manore, L. Weir, K. Wilson and D. Bradley (1998). '*Utilization of RADARSAT Data in the Canadian Ice Service.*' Application Development and Research Opportunity (ADRO) Symposium, Montreal, October

Randell, C., M. Rokonuzzaman, J. Youden and R. Khan (1998). '*Evaluation of RADARSAT for Detection, Classification and Discrimination of Icebergs.*' Application Development and Research Opportunity (ADRO) Symposium, Montreal, October

Schuh et al, (2002). '*Prediction of Earth Orientation Parameters by Artificial Neural Networks.*' Journal of Geodesy, Vol. 76, pp. 247-258

E-mail: rabbany@ryerson.ca